



Original Article

Application of tetracycline hydrochloride loaded-fungal chitosan and *Aloe vera* extract based composite sponges for wound dressing

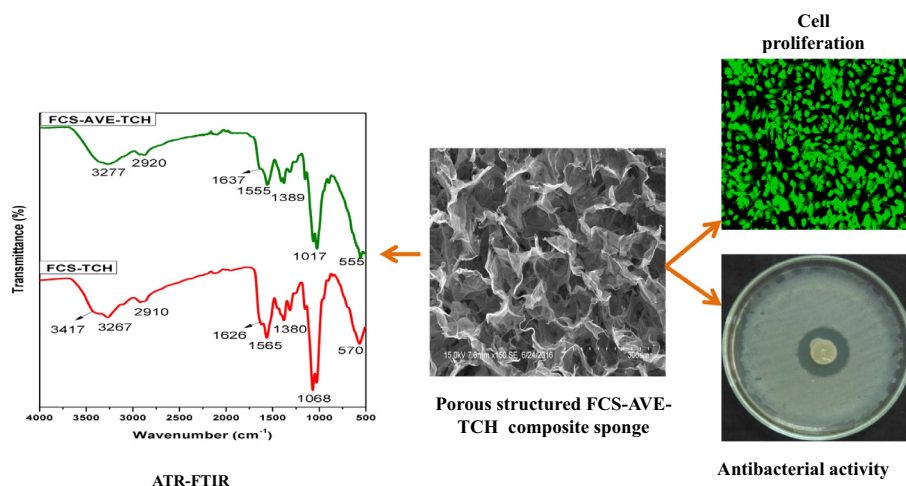
Sathiyaseelan Anbazhagan^{a,*}, Kalaichelvan Puthupalayam Thangavelu^{a,b}

^a Centre for Advanced Studies in Botany, University of Madras, Guindy Campus, Chennai, Tamil Nadu, India

^b Alka Research Foundation, Maruthamalai Adivaaram, Coimbatore, Tamil Nadu, India



GRAPHICAL ABSTRACT



ARTICLE INFO

Article history:

Received 6 February 2018

Revised 7 May 2018

Accepted 8 May 2018

Available online 14 May 2018

Keywords:

Fungal chitosan

Aloe vera extract

Tetracycline hydrochloride

Wound dressing

ABSTRACT

Chitosan composite material has been used as an efficient drug carrier for potential drug delivery systems in specific cases of wound dressing management. In the present study, 0.5 g/L of the antibiotic tetracycline hydrochloride (TCH) was loaded into 1% fungal chitosan (FCS) incorporated with 0.2% of *Aloe vera* extract (AVE). Two types of sponges were prepared, with and without AVE, such as FCS-AVE-TCH and FCS-TCH, respectively. They were characterized by UV–Visible spectrophotometer, attenuated total reflectance Fourier transform infrared spectroscopy (ATR-FTIR), and scanning electron microscopy (SEM). A constant amount of cumulative TCH release was observed from FCS-AVE-TCH composite sponges at the phosphate buffer saline (pH 7.4), they exhibited good antibacterial activity against both Gram-positive and Gram-negative bacteria. Furthermore, the Vero cells (African green monkey kidney cell line) treated by the composites showed augmented cell viability, which suggests that it could be used as a cost-effective, potential wound dressing material.

© 2018 Production and hosting by Elsevier B.V. on behalf of Cairo University. This is an open access article under the CC BY-NC-ND license (<http://creativecommons.org/licenses/by-nc-nd/4.0/>).

Peer review under responsibility of Cairo University.

* Corresponding author at: Nanobiotechnology Lab, Guindy Campus, CAS in Botany, University of Madras, 600025 Tamil Nadu, India.

E-mail address: sathiyaseelan.bio@gmail.com (S. Anbazhagan).

Introduction

Currently, chitosan and chitosan derivatives-based composite materials are used widely in drug delivery applications [1,2].

<https://doi.org/10.1016/j.jare.2018.05.005>

2090-1232/© 2018 Production and hosting by Elsevier B.V. on behalf of Cairo University.

This is an open access article under the CC BY-NC-ND license (<http://creativecommons.org/licenses/by-nc-nd/4.0/>).

Because of their various physicochemical properties, such as biodegradability, mucoadhesion, and biocompatibility [3–5], these polymers have shown a unique nature compared to other polymers. Chitosan (β -(1-4)-2-amino-2-deoxy-d-glucose) is a deacetylated product of the linear polysaccharide chitin, which is the second most abundant natural polymer in the world after cellulose and is commonly found in the shells of marine crustaceans and cell walls of fungi [6–8]. The difficulties in isolating marine sources based chitosan obtained from fungal sources have been overcome; for instance, removal of proteins, calcium content, and pigments have been reported [8,9].

Wound healing is a complex process [10–12] where microbial infection can worsen the healing process [13,14]. The drug-loaded porous structured biomaterials are able to overcome all the issues in wound healing [15]. Chitosan sponges have been reported to have the potential for wound healing and subcutaneous implantation of the delivered drugs, proteins, growth factors, vitamins, minerals, fibroblasts, and platelets [16–20]. However, it is expensive for people living in low-income countries.

The ultimate aim of the current study was to produce inexpensive, reproducible, and efficient wound dressing material. Accordingly, fungal chitosan, *Aloe vera* extract (AVE), and tetracycline hydrochloride (TCH) were chosen for the present study. In the previous work, silver nanoparticles loaded with FCS-AVE nanocomposite sponges exhibited good antibacterial and cell proliferation activities. Moreover, AVE incorporated composites minimized silver toxicity and exhibited synergistic activity with chitosan to enhance the proliferation of human dermal fibroblast cells [21]. *Aloe vera* is a natural therapeutic plant that has been used for wound healing and against burning and inflammatory activity [22]. In view of the significant amount of amino acids, glycoproteins, and other antioxidant molecules in *Aloe vera*, cell proliferation increases [23]. TCH is a well-known antibiotic that controls bacterial growth by way of inhibiting enzymatic reactions, protein and ribosome synthesis, and altering the cytoplasmic membrane synthesis. Because of these benefits, TCH is still being used in wound dressing materials [24,25].

With this background, the fungal chitosan-based FCS-TCH and FCS-AVE-TCH composites were developed, their physicochemical properties evaluated, antibacterial activity and *in vitro* drug release studied. In addition, the composites were analyzed *in vitro* drug release to the Vero cells with respect to their response to wound dressing materials.

Material and methods

Material

Tetracycline hydrochloride (TCH) and Muller Hinton agar (MHA) were purchased from HiMedia Laboratories (Mumbai, India); MTT (3-(4,5-Dimethyl-2-thiazolyl)-2,5-diphenyl tetrazolium Bromide), acridine orange (AO) and ethidium bromide (EB) was procured from Sigma Aldrich (Mumbai, India); Sodium hydroxide and Lysozyme were obtained from Sisco Research Laboratories Pvt. Ltd. (Chennai, India); Acetic acid (AA) was procured from SD Fine Chem Limited (Chennai, India). All the chemicals were used without further purification. The low molecular weight fungal chitosan, with the degree of deacetylation 80.85%, was isolated from the fungus *Cunninghamella elegans* [21].

Preparation of FCS-TCH and FCS-AVE-TCH composite sponges

Fungal chitosan (0.5 g) was dissolved in 50 mL of 1% acetic acid solution. Then 0.5 g/L of aqueous soluble TCH was added into the fungal chitosan (FCS) solution under continuous stirring

(800 rpm) for 5 h and the FCS-TCH composite solution was prepared. Preparation of AVE and FCS-AVE composites has been discussed in previous studies [21]. In brief, 0.2% of AVE was added drop-wise into the completely dissolved FCS solution stirring continuously for 2 h, and subsequently, the TCH solution was added. The stirring was continued for another 5 h. The one milliliter of composite solution was then poured into a 24-well plate (15.5 dia. x 18 deep mm), freeze at -50°C , lyophilized (FD-10 M Freeze Dryer, LARK, India), and the sponges obtained (15.5 dia. x 10 mm height) were kept at -20°C until further use.

Characterization

The FCS, TCH, AVE, FCS-TCH, FCS-AVE, and FCS-AVE-TCH composite solutions were examined under UV-Visible spectroscopy at a spectral range of 200–700 nm. The functionalities of all the composite sponge materials were recorded by using FTIR-ATR spectrometer (PerkinElmer-spotlight 400 FT-IR Imaging system, India) with a spectral range of 4000–450 cm^{-1} . Furthermore, the gold sputter coated composite sponges were observed with a scanning electron microscope (Hitachi S3400, Japan), precision at 15.0 keV.

Porosity measurement

The porosity of fungal chitosan-based composite sponge was analyzed by the liquid displacement method using ethanol [37]. A Vernier caliper was used to measure the dimensions of the sponges and the volume (V) was calculated. The initial weight (W_i) of the lyophilized sponges were recorded, and they were immersed into a known volume of ethanol in a graduated cylinder for 24 h, and the final weight (W_f) of the wet sponges was recorded. Accordingly, porosity was calculated using Eq. (1). The experimental data were obtained in triplicate and the results were shown in mean \pm standard deviation ($n = 3$).

$$\% \text{ of porosity} = \left(\frac{W_f - W_i}{(\rho_{\text{ethanol}} \times V)} \right) \times 100 \quad (1)$$

ρ_{ethanol} : density of ethanol.

Water sorption and moisture retention capacity

Water sorption capacity of FCS-TCH and FCS-AVE-TCH sponges were evaluated at different time intervals, viz., 1 h, 2 h, 3 h, 4 h, 5 h, and 6 h in deionized water at room temperature. All the dry sponges (W_d) were pre-weighed and then immersed into the buffer solution, the wet sponges (W_w) were weighed at each interval, and the excess amount of water was gently removed by using tissue paper. The experiment was performed thrice. The following formula (2) was used to calculate the water sorption capacity. The results were expressed as the mean \pm standard deviation ($n = 3$).

$$\% \text{ of water sorption} = \frac{W_w - W_d}{W_d} \times 100 \quad (2)$$

For evaluating the moisture retention capacity, the composite sponges were evaluated using the procedure as detailed by Liang et al. [36]. In brief, the dry sponges (W_d) were immersed in deionized water for 2 h, and the wet sponges (W_w) were placed in a glass petri dish at the room temperature. The moisture retention capacity was recorded each hour up to reaching their dry weight. The results were expressed as the mean \pm standard deviation ($n = 3$).

Blood absorption assay

Blood absorption assay was carried out according to Hajosch et al. 2009 [38] with some modification. In brief, the erythrocyte

was isolated from human blood and was stabilized with citrate-phosphate-dextrose with adenine solution, and then it was diluted with an isotonic saline solution (1:4 ratio). The 40–56% of red blood cells was used for blood absorption assay. The sponges were gently introduced into the blood surface for 20 s. Subsequently, the sponges that had absorbed the blood were placed on the Whatman filter paper grade 1 (Sigma Aldrich, Mumbai, India) for 1 min to remove the excess amount of blood. The sponges were weighed before being introduced to the blood (M_d) and after removing excess amount of blood (M_w). Blood absorption capacity (BAC) was calculated by the formula in Eq. (3). The experiment was repeated thrice and the data were expressed as the mean \pm standard deviation ($n = 3$).

$$BAC = \frac{M_w - M_d}{M_d} \quad (3)$$

Biodegradation assay

The biodegradation (BD) of FCS-AVE-TCH composite sponge was determined by Su et al. 2017 [39] with some modification. In brief, the FCS-AVE-TCH sponges were immersed into the PBS solution (pH = 7.4) containing 50 $\mu\text{g}/\text{mL}$ of lysozyme enzyme (15,000 U/mg) at 37 °C for 15 days. At each predetermined interval (5, 10, and 15 days), the immersed sponges were taken out, washed with deionized water, and freeze-dried. The biodegradability of FCS-AVE-TCH sponges was calculated using Eq. (4).

$$BD = \frac{(W_0 - W_t)}{W_0} \times 100\% \quad (4)$$

where W_0 was the initial weight of FCS-AVE-TCH, and the weight after freeze-drying was (W_t). The degradation percentage was expressed as the mean \pm standard deviation ($n = 3$).

In vitro drug release

To determine the TCH release from FCS-TCH and FCS-AVE-TCH, the composite sponges were immersed in a dissolution bath containing 20 mL Phosphate buffer (pH 7.4) at 37 °C under shaking condition (200 rpm). At predetermined time intervals (10, 20, 30, 40, 50, 60, 120, 180, 240, 300, and 360 min) 2 mL of samples were drawn from the dissolution bath and an equal amount of fresh buffer was replaced each time to maintain the equilibrium constant. The volume of the drawn sample was examined with a UV-Visible spectrophotometer at an absorbance of 356 nm and the results recorded. The concentration of TCH release was calculated using the linear curve to obtain values from known concentrations of TCH. The cumulative drug release percentage was calculated and expressed as the mean \pm standard deviation ($n = 3$). The obtained data were fitted with various mathematical models for drug release, such as zero order, first order, Korsmeyer–Peppas, Hixson–Crowell, and Higuchi models, as followed by Dhanavel et al. 2017 [26].

In vitro antibacterial activity

The antibacterial activity of fungal chitosan and composite sponges were tested against both the Gram-positive (*Staphylococcus aureus* ATCC 33592 and *Bacillus subtilis* ATCC 55614) and Gram-negative bacteria (*Klebsiella pneumoniae* ATCC 13884 and *Escherichia coli* ATCC 11229). The bacterial cultures were incubated in freshly prepared nutrient broth medium at 37 °C overnight. The adjusted bacterial suspensions (10^7 cells/mL) were uniformly spread on an MHA plate; then the various composite sponges were placed on the bacteria inoculated plates and incubated overnight at 37 °C. After incubation, the zone of inhibition around the compos-

ite sponges was measured in terms of millimeters. The experiment was done in triplicate, the data were expressed as the mean \pm standard deviation ($n = 3$).

In vitro cell viability and observation of cell morphology

The FCS and composites-treated Vero cells were tested for cell viability by using MTT assay. The Vero cells were grown in DMEM medium supplemented with 10% FBS and antibiotics, penicillin (100 $\mu\text{g}/\text{mL}$) and Streptomycin (100 $\mu\text{g}/\text{mL}$). The 200 μL of Vero cells (1×10^5) were seeded on a 96-well plate, incubated in a humidified chamber overnight at 37 °C with an atmosphere containing 5% CO_2 , and the media were discarded. Twenty μL of FCS, TCH, AVE, FCS-TCH, FCS-AVE, and FCS-AVE-TCH were added to each well of the plate, and the plates were incubated for 24 h. For the control, the cells were maintained without any of the above-mentioned components. The samples containing the media were changed and fresh media used, 20 μL of MTT was added to each well, and the incubation continued for 6 h. After that, the medium was removed and 200 μL DMSO was added to each well to dissolve the formazan, and then the plates were measured at an absorbance of 570 nm to calculate the percentage of cell viability. Furthermore, the Vero cells seeded on a 6-well plate were treated with the composites mentioned earlier, and the morphology of the cells was observed (20X magnification) under a fluorescence microscope (EVOS Fluid cell imaging station, Thermo Fisher Scientific – USA) by using the dual staining (AO/EB) technique [27].

Statistical analysis

All the experimental data were expressed as means \pm SD. The cell viability data were analyzed using one-way analysis of variance (ANOVA) with Prism software 6.00 (Graph Pad Software for Windows, La Jolla, CA, USA), followed by Dunnett's post hoc test to depending on the homogeneity of the variance test. In this experiment, $P < 0.05$ was considered statistically significant. The antibacterial activity was examined using the one way ANOVA and the least significant difference was at 5%. These tests were used to compare the means of the zone using the IBM SPSS version 20.1 (IBM SPSS statistics for windows, version 22.0. Armonk, NY: IBM Corp).

Results and discussion

Characterization of composites

Fig. 1a shows the UV-Visible spectra of the composites; the FCS shows absorption peaks at 200–205 nm assigned to the $\pi \rightarrow \pi^*$ transition [28]. The absorption spectrum of TCH exhibited three absorption peaks at 218, 273, and 356 nm corresponding to $\pi \rightarrow \pi^*$, $\pi \rightarrow \pi^*$, and $n \rightarrow \pi^*$ transitions [29]. AVE showed absorbance peaks at 290 and 350 nm corresponding to $\pi \rightarrow \pi^*$ and $n \rightarrow \pi^*$ transitions. The absorption peak of the FCS-AVE combination appeared at 230 nm. The FCS-TCH combination showed all the respective peaks of TCH with lower intensity. The combination of FCS-AVE-TCH exhibits absorption peaks at 230 nm along with the TCH peaks (Fig. 1a), which shows that all the major functional groups were present in the composites.

Attenuated total reflectance Fourier transform infrared spectroscopy (ATR-FTIR)

The ATR-FTIR spectra of FCS, TCH, AVE, FCS-AVE, FCS-TCH, and FCS-AVE-TCH are shown in the Figs. 1b and 1c. The fungal chitosan spectra showed the characteristic band at 1637 cm^{-1} , assigned to

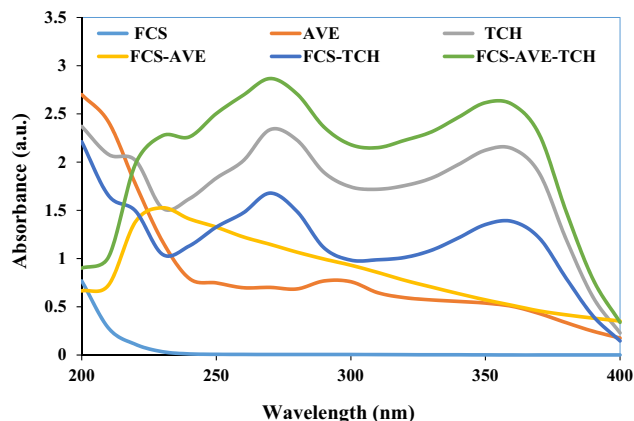


Fig. 1a. UV-Visible spectrum. FCS – Fungal chitosan, TCH – Tetracycline hydrochloride, AVE – *Aloe vera* extract, and the combination of FCS-TCH, FCS-AVE, FCS-AVE-TCH composites.

C=O stretching frequency, the N–H bending frequency at 1555 cm^{-1} assigned to the amine and amide II bands, and the medium intensity bands at 3406 cm^{-1} and 3273 cm^{-1} attributed to –OH and –NH stretching frequency [8,30]. The FTIR spectrum of tetracycline shows the characteristic peak at 1660 cm^{-1} corresponding to the amide carbonyl group. The appearance of a doublet at 1601 cm^{-1} and 1610 cm^{-1} accounted for the N–H bending frequency, with the N–H band appending with the O–H band at $3300\text{--}3313\text{ cm}^{-1}$ [31,32]. The AVE spectrum exhibited the band at 3344 cm^{-1} , attributed to the N–H stretching frequency. A weak band at 2926 cm^{-1} is assigned to CH stretching frequency, and the sharp band that appears at 1611 cm^{-1} indicates the presence of the carbonyl groups. The spectra of FCS-TCH and FCS-AVE-TCH composite are shown in Fig. 1c. When TCH and AVE were added to fungal chitosan, the ATR spectra did not exhibit any substantial changes, because the concentrations of the TCH and AVE were low and evenly assimilated into the composite sponge. The PVA/Chitosan/Tetracycline hydrochloride wound dressing mats did not show any significant difference in ATR spectra [25]. The results suggest that the amide group of the fungal chitosan are responsible for the formation of the intermolecular hydrogen bonding.

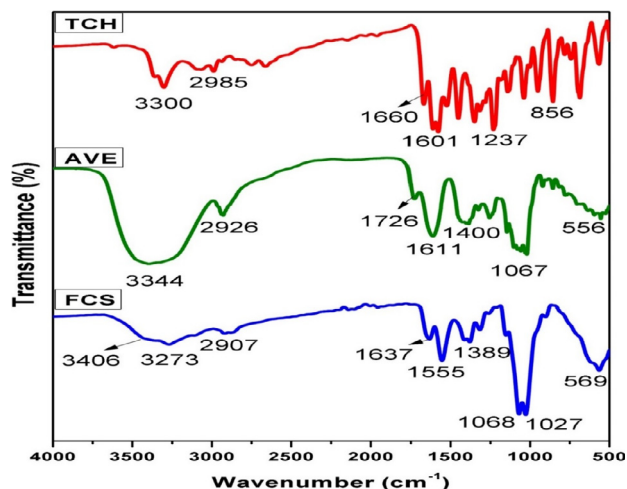


Fig. 1b. FTIR – ATR Spectra of TCH – Tetracycline hydrochloride, AVE – *Aloe vera* extract and FCS – Fungal chitosan.

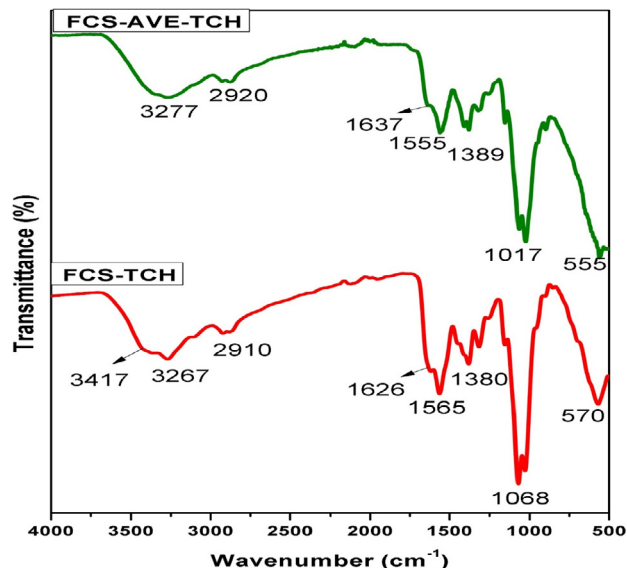


Fig. 1c. FTIR – ATR spectra of FCS-AVE-TCH – Fungal chitosan incorporated *Aloe vera* extract bounded Tetracycline hydrochloride and FCS-TCH – Fungal chitosan bounded tetracycline hydrochloride.

SEM analysis

The SEM image of FCS and FCS-reinforced composite sponges are shown in Fig. 2. The porous structure of the FCS sponge was shown to be compact, whereas TCH added FCS-TCH composite sponges displayed less compact porous structure. The AVE added FCS-AVE-TCH sponge as present in the well-interconnected porous structure is shown in Fig. 2. The results exhibit that AVE promotes the formation of the porous structure without destruction.

Porosity measurement

The porosity of the composite sponges was evaluated by the liquid displacement method. FCS and FCS-TCH sponges showed porosity of 56.44% and 55.87%, respectively. FCS-AVE-TCH sponges had a porosity of 68.74%, which was higher than the control sponges (Fig. 3a). Hence, the higher the porosity in the FCS-AVE-TCH composite, the more the AVE extract can bind with the free amine and hydroxyl groups of chitosan as shown by the ATR-FTIR spectral analysis. The development of fungal chitosan and *Aloe vera* extract-based antibacterial drug loaded wound dressing composite sponges have the advantages of a porous structured morphology that helps in enhancing the gaseous exchange and absorption of wound exudates [36] by the way it releases active molecules to the wounded skin.

Water sorption and moisture retention capacity

Water sorption is a significant characteristic of good wound dressing material where it has to absorb the water that the wound exudates and further release the drug in an osmotic manner. Fungal chitosan sponges exhibited good sorption capacity (Fig. 3b). At the 4th h, FCS-TCH and FCS-AVE-TCH sponges showed 1476.73% and 1652.73% sorption capacity, respectively; furthermore, the amount of absorption was maintained until the end of the experiment. The water absorption behavior of composite sponges increased with respect to increasing time, and a constant amount was maintained after reaching the equilibrium constant. The swelling behavior of wound dressing materials depending on the poros-

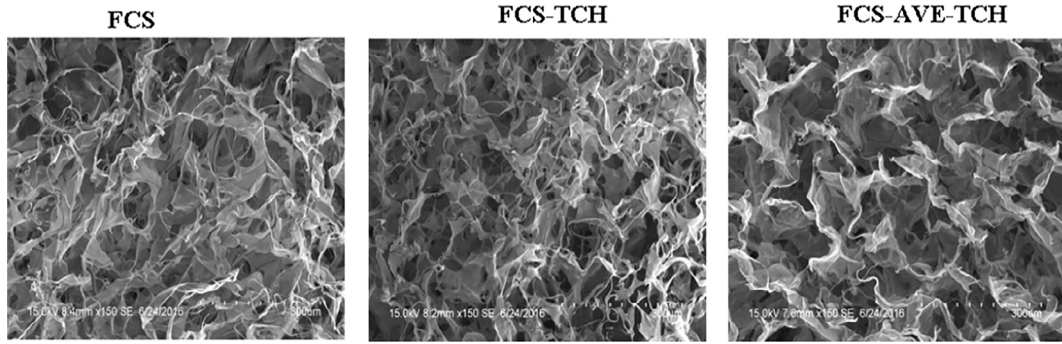


Fig. 2. SEM image of porous structured sponges.

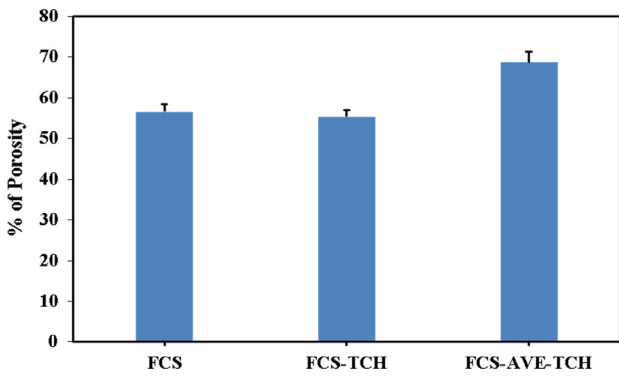


Fig. 3a. Porosity of fungal chitosan and fungal chitosan composite sponges.

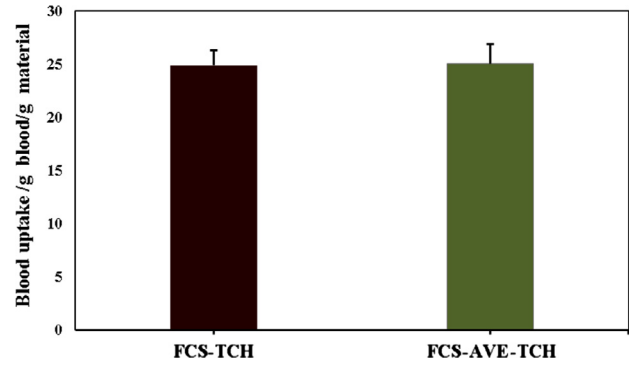


Fig. 3d. *In vitro* blood absorption capacity of fungal chitosan based composite sponges FCS-TCH and FCS-AVE-TCH.

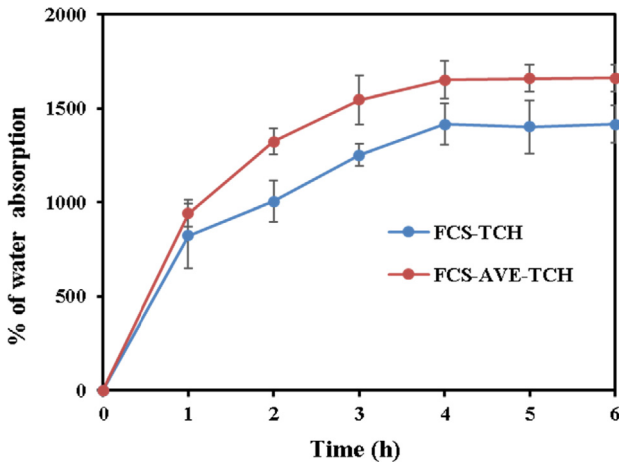


Fig. 3b. Percentage of water sorption capacity of composite sponges.

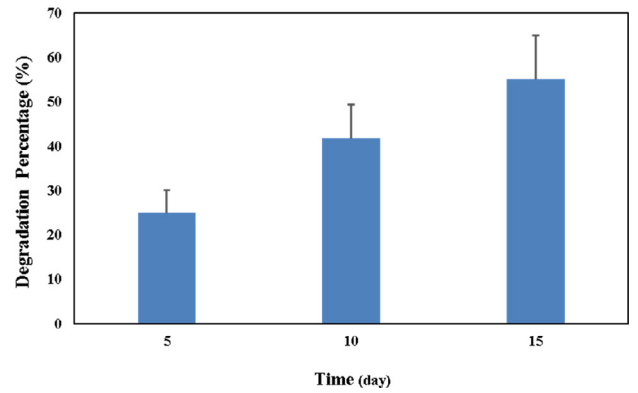


Fig. 3e. *In vitro* degradation of FCS-AVE-TCH composite sponge.

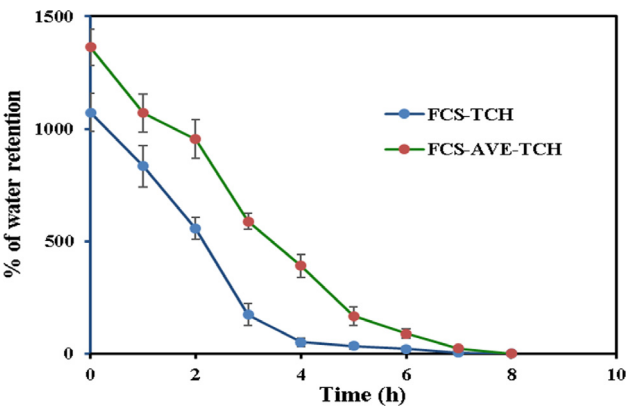


Fig. 3c. Percentage of water retention capacity of composite sponges.

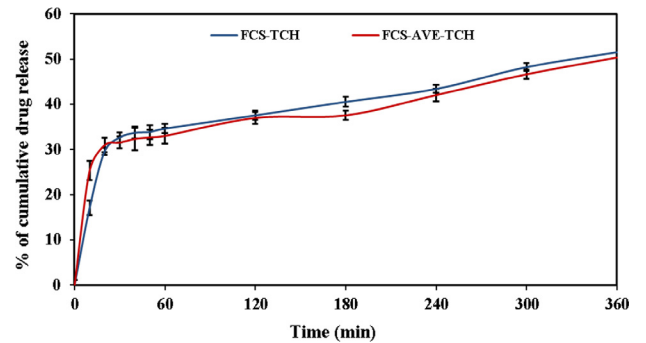


Fig. 3f. Tetracycline hydrochloride cumulative release of FCS-TCH and FCS-AVE-TCH composite sponges.

ity and the highly porous material's absorption rate was higher than the material with low porosity.

The FCS-TCH and FCS-AVE-TCH sponges were tested for their moisture retention capacity (Fig. 3c). The FCS-TCH and FCS-AVE-TCH composites sponges attained their own dry weight at 6 and

8 h, respectively. The moisture retention capacity was different at each hour between the two composite sponges. The FCS-AVE-TCH had a better organized porous structure than the FCS-TCH sponges, seen in the different initial absorption capacity of the sponges (Fig. 3c).

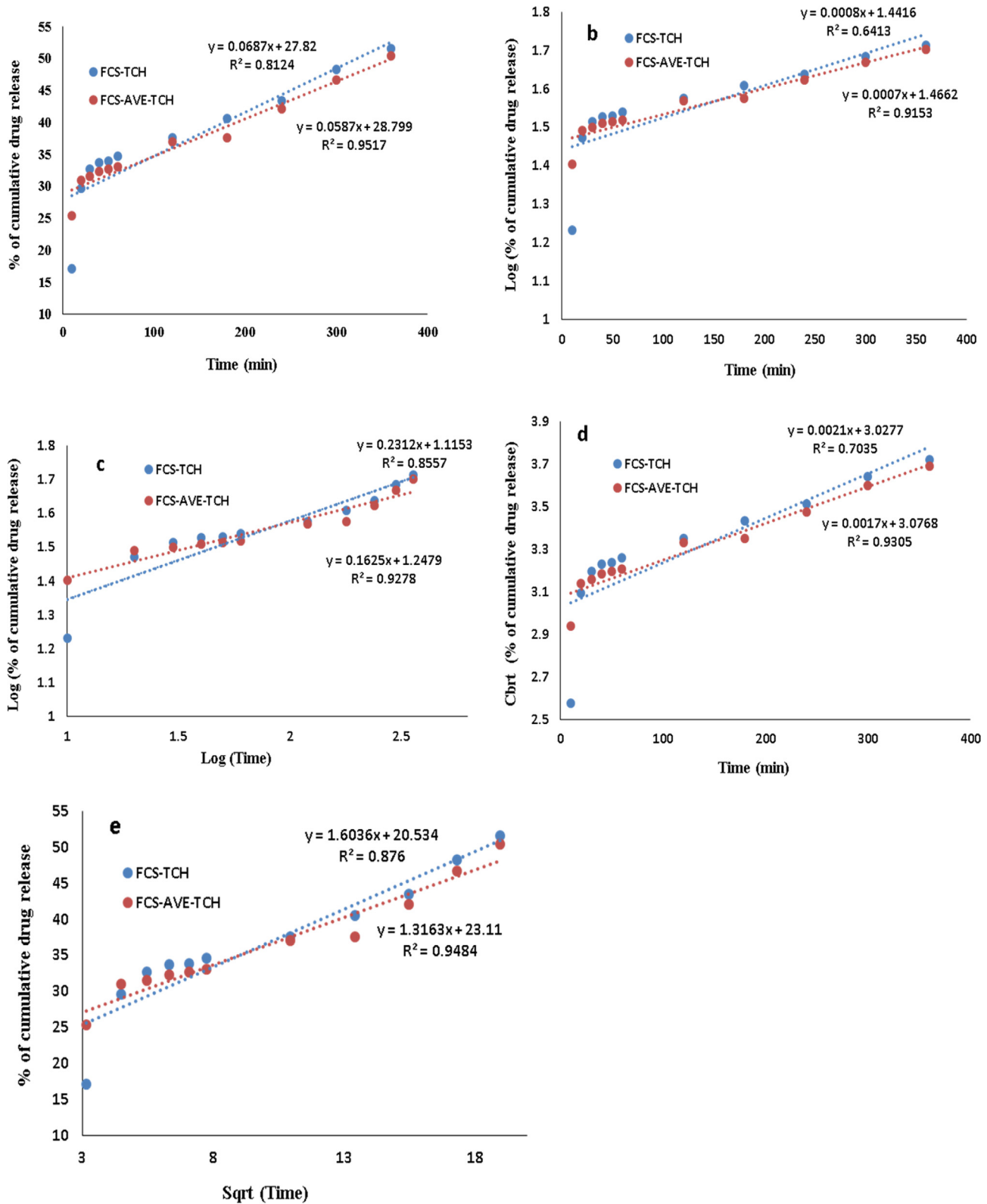


Fig. 4. Fitting of drug release to the different kinetic model. Zero order – a, First order – b, Korsmeyer-Peppas-c, Hixson-Crowell – d and Higuchi – e.

Blood absorption assay

The FCS-TCH and FCS-AVE-TCH composite sponges were tested *in vitro* against red blood cells (RBC) by absorption assay (Fig. 3d). It was observed that FCS-TCH sponges absorbed 24.88 times its own weight, whereas the FCS-AVE-TCH sponges absorbed 25.08 times its own weight. Blood uptake capacity of the sponges would be helpful in avoiding blood loss at the time of bleeding and also promote the blood flow between the wound skins [38]. However, the developed sponges had not absorbed the blood like deionized water and need further detailed optimization and studies.

Biodegradation of FCS-AVE-TCH sponges

The biodegradation property of FCS-AVE-TCH sponges was evaluated with lysozyme as shown in Fig. 3e. The biodegradation rate of sponges was 25% (5th day), 41.6% (10th day), and

55% (15th day). The FCS-AVE-TCH sponges have shown good biodegradable property, which could be used for wound dressing application.

In vitro drug release

Fig. 3f shows that the accumulated TCH release from FCS-TCH and FCS-AVE-TCH sponges during the 6 h under *in vitro* condition.

The TCH release was increasing gradually from the composite with respect to increasing the time due to the strong hydrophilic affinity of the drug [25]. The drug release profile from the polymeric matrix was fitted with various mathematical models, such as zero order, first order, Korsmeyer–Peppas, Hixson–Crowell, and Higuchi models, as shown in Fig. 4(a)–(e). The TCH release was determined by the R squared value obtained from the kinetic fitting of drug release, and based on the highest regression coefficient, the better drug release kinetic model was proposed. Both the FCS-TCH and FCS-AVE-TCH sponges initially exhibited 17% and 25% in drug release due to the swelling of the polymer composite and enhanced the diffusion of the drug, which is present on the surface of the composites [26].

The TCH release from the FCS-TCH composite was best fitted with the Higuchi model ($r^2 = 0.876$) compared to the others, and FCS-AVE-TCH composite was best fitted with zero order release ($r^2 = 0.951$) and the Higuchi model ($r^2 = 0.948$), whereas the release of the water-soluble drug was better fitted with the Higuchi model [33]. The TCH release from FCS-AVE-TCH composite did not show significant difference among the kinetic drug release models, and it does release the drug by diffusion and swelling mechanisms. The TCH release of FCS-AVE-TCH fitted with the specifically developed drug release kinetic model (Korsmeyer–Peppas) from the polymer matrix showed the R^2 value at 0.9278. The release exponent ($n = 0.162$) indicated a Fickian diffusion; the previous reports of PVA and

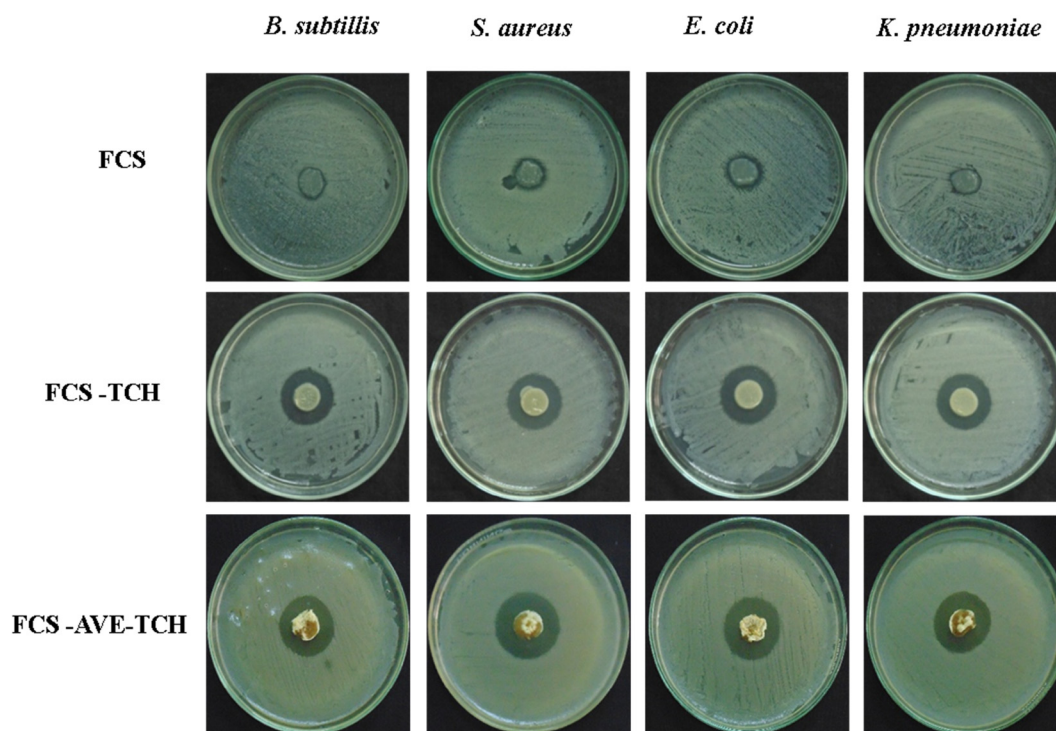


Fig. 5. Photographic image of chitosan and composites sponges antibacterial activity.

Table 1
Antibacterial activity of fungal chitosan and fungal chitosan composite sponges.

	<i>Bacillus subtilis</i>	<i>Staphylococcus aureus</i>	<i>Escherichia coli</i>	<i>Klebsiella pneumoniae</i>
Zone of inhibition in millimeter				
FCS	17.03 ± 0.65 ^b	19 ± 1 ^a	18.5 ± 0.82 ^{ab}	15.7 ± 1.26 ^c
FCS-TCH	20.0 ± 1.4 ^d	22.0 ± 1.4 ^c	26.17 ± 1.53 ^a	24.5 ± 0.5 ^b
FCS-AVE-TCH	27.0 ± 0.5 ^b	28.0 ± 0.6 ^a	27.53 ± 0.50 ^{ab}	27.0 ± 1 ^b

Values represent the mean ± SD of three replicates. Values followed by uppercase letters in a column are significant differences ($P < 0.05$) among the groups.

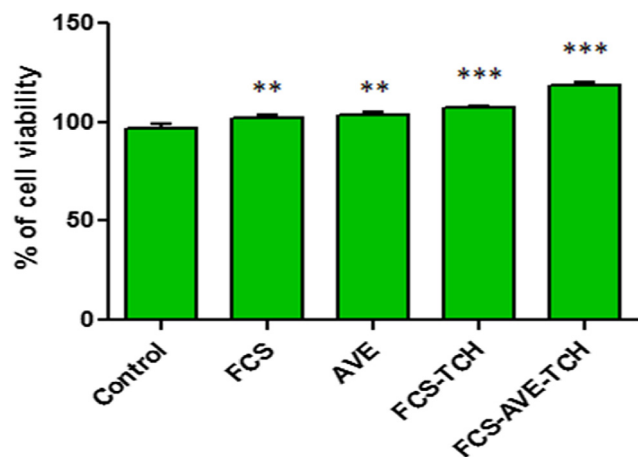


Fig. 6a. Cell viability (%) of Chitosan composite sponges treated Vero cells. Fungal Chitosan (FCS), *Aloe vera* extract (AVE), Fungal chitosan and *Aloe vera* extract (FCS-AVE), Fungal chitosan and *Aloe vera* extract with Tetracycline hydrochloride (FCS-AVE-TCH). Values are expressed mean \pm SD. Each experiments were repeated thrice, *** $P < 0.001$ (Control vs FCS-AVE-TCH) and (Control vs FCS-TCH), ** $P < 0.01$ (Control vs FCS) and (Control vs AVE).

chitosan-based nanofiber matrix also reported the release of TCH in the same manner [25]. With this background, the FCS-AVE-TCH composite sponges released the drug in a constant manner, which is good for wound dressing applications.

In vitro antibacterial activity

FCS, FCS-TCH, and FCS-AVE-TCH sponges were tested for antibacterial activity against Gram-positive and Gram-negative bacteria. FCS sponges showed lesser inhibitory actions against both the bacteria. But the FCS-TCH and FCS-AVE-TCH sponges exhibited maximum inhibitory action against *Bacillus subtilis*, *Staphylococcus aureus*, *Escherichia coli*, and *Klebsiella pneumoniae*

by way of antibiotic drug release. Comparatively, the FCS-AVE-TCH sponges displayed substantial activity in terms of the zone of inhibition, with 27 ± 0.5 mm, 28 ± 0.6 mm, 27.53 ± 0.50 mm, and 27 ± 1.0 mm, respectively (Fig. 5 and Table 1). The FCS sponges showed inhibitory activity against both Gram-positive and Gram-negative bacteria because of the low molecular weight of chitosan [14,21,34]. Further, the FCS-TCH and FCS-AVE-TCH sponges exhibited substantial antibacterial activity because of TCH, which is a well-established antibacterial drug [13]. Moreover, microporous structured sponges enhanced the antibacterial activity by the mechanism of absorbing of water and releasing of the antibacterial drugs through the diffusion process [40].

In vitro cell viability

To determine the cell viability of FCS, FCS-TCH, and FCS-AVE-TCH composites treated with Vero cells, FCS-TCH and FCS-AVE-TCH composites were evaluated using *in vitro* studies, and they revealed that both the composites and individual constituents did not show any decreasing percentage of cell viability compared with control; instead, they increased the proliferation of cell numbers. This study also proved that the 0.5 g/L TCH loaded FCS (1%)-AVE (0.2%) did not induce any toxicity, while it maintained higher cell viability and also increased cell proliferation compared to control (Fig. 6a).

In addition, the morphological changes of Vero cells were evaluated by the dual staining (AO/EB) technique under the fluorescence microscope. The results showed that the cells had no changes in morphology when observed under a fluorescent microscope. After the treatment with the composites, the cell viability was significantly increased when compared to control (Fig. 6b). The FCS-TCH composites were nontoxic to the normal cells but completely inhibited bacterial development. The bacterial cellulose composites delivered 0.5 g/L of tetracycline hydrochloride to the HEK293 cell line, and no adverse effects were observed [35].

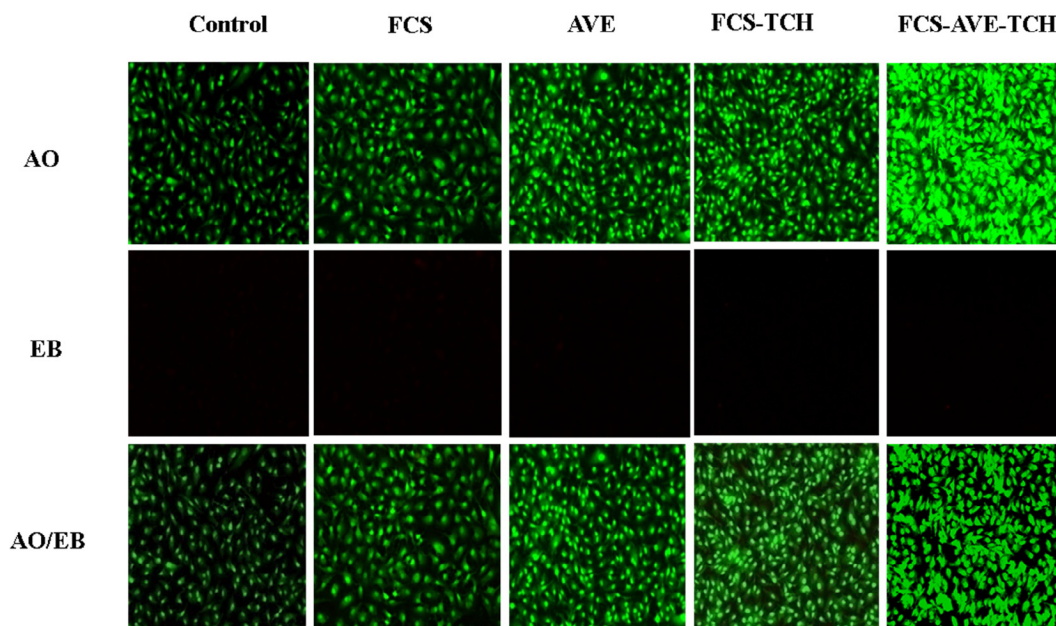


Fig. 6b. Morphological observation Fungal Chitosan (FCS), *Aloe vera* extract (AVE), Fungal chitosan and *Aloe vera* extract (FCS-AVE) and Fungal chitosan, *Aloe vera* extract with Tetracycline hydrochloride (FCS-AVE-TCH) composites treated Vero cells staining with AO/EB and observed under fluorescence microscope with 20 \times magnification.

Conclusions

Porous, micro-fibrous structure composite sponges were prepared with a fungal chitosan- reinforced *Aloe vera* extract and associated with tetracycline hydrochloride. The composite sponges delivered antibiotic by way of *in vitro* drug delivery efficiently and displayed *in vitro* antibacterial activity while enhancing cell proliferation with the help of the natural wound healing agent AVE. Based on the review of the literature, a porous structured chitosan composite will enhance wound healing property by way of proper oxygen supply, good absorption of wound exudates, and enhancement of epidermal growth factor. Hence, these findings indicate that the FCS-AVE-TCH sponges could be used as a potential cost-effective wound dressing material.

Conflict of interest

The authors have declared no conflict of interest.

Compliance with Ethics Requirements

This article does not contain any studies with human or animal subjects.

Acknowledgments

The author (A. S) thank the University Grants Commission (UGC), New Delhi, India for providing research fellowship under the UGC-BSR scheme. The authors also grateful to the Director Prof. N. Mathivanan, CAS in Botany, University of Madras – India for providing laboratory facilities.

References

- Patrulea V, Ostafe V, Borchard G, Jordan O. Chitosan as a starting material for wound healing applications. *Eur J Pharm Biopharm* 2015;97:417–26.
- Ahmed S, Ikram S. Achievements in the life sciences chitosan based scaffolds and their applications in wound healing. *ALS* 2016;10:27–37.
- Tharanathan RN, Kittur FS. Chitin—the undisputed biomolecule of great potential. *Crit Rev Food Sci Nutr* 2003;43:61–87.
- Kasaai MR. Various methods for determination of the degree of N-acetylation of chitin and chitosan: a review. *J Agric Food Chem* 2009;57:1667–76.
- Jayakumar R, Prabaharan M, Sudheesh Kumar PT, Nair SV, Tamura H. Biomaterials based on chitin and chitosan in wound dressing applications. *Biotechnol Adv* 2011;29:322–37.
- Kurita K. Chemistry and application of chitin and chitosan. *Polym Degrad Stab* 1998;59:117–20.
- Pochanavanich P, Suntornsuk W. Fungal chitosan production and its characterization. *Lett Appl Microbiol* 2002;35:17–21.
- Wu T, Zivanovic S, Draughon FA, Sams CE. Chitin and chitosan—value-added products from mushroom waste. *J Agric Food Chem* 2004;52:7905–10.
- Wang WP, Du YM, Wang XY. Physical properties of fungal chitosan. *World J Microbiol Biotechnol* 2008;24:2717–20.
- Boateng JS, Matthews KH, Stevens HNE, Gillian M. Eccleston. wound healing dressings and drug delivery systems: a review. *J Pharm Sci* 2008;97:2892–923.
- Muzzarelli RAA. Chitins and chitosans for the repair of wounded skin, nerve, cartilage and bone. *Carbohydr Polym* 2009;76:167–82.
- Muzzarelli RAA, Boudrant J, Meyer D, Manno N, DeMarchis M, Paoletti MG. Current views on fungal chitin/chitosan, human chitinases, food preservation, glucans, pectins and inulin: a tribute to Henri Braconnot, precursor of the carbohydrate polymers science, on the chitin bicentennial. *Carbohydr Polym* 2012;87:995–1012.
- Chopra I, Roberts M. Tetracycline antibiotics: mode of action, applications, molecular biology, and epidemiology of bacterial resistance. *Microbiol Mol Biol Rev* 2001;65:232–60.
- Shen E-C, Wang C, Fu E, Chiang C-Y, Chen T-T, Nieh S. Tetracycline release from tripolyphosphate – chitosan cross-linked sponge: a preliminary *in vitro* study. *J Periodontol Res* 2008;642–8.
- Wang QZ, Chen XG, Liu N, Wang SX, Liu CS, Meng XH, et al. Protonation constants of chitosan with different molecular weight and degree of deacetylation. *Carbohydr Polym* 2006;65:194–201.
- Dai M, Zheng X, Xu X, Kong X, Li X, Guo G, et al. Chitosan-alginate sponge: preparation and application in curcumin delivery for dermal wound healing in rat. *J Biomed Biotechnol* 2009;1:–8.
- Noel SP, Courtney HS, Bumgardner JD, Haggard WO. Chitosan sponges to locally deliver amikacin and vancomycin: a pilot *in vitro* evaluation. *Clin Orthop Relat Res* 2010;468:2074–80.
- Anisha BS, Sankar D, Mohandas A, Chennazhi KP, Nair SV, Jayakumar R. Chitosan-hyaluronan/nano chondroitin sulfate ternary composite sponges for medical use. *Carbohydr Polym* 2013;92:1470–6.
- Mohandas A, Anisha BS, Chennazhi KP, Jayakumar R. Chitosan-hyaluronic acid/VEGF loaded fibrin nanoparticles composite sponges for enhancing angiogenesis in wounds. *Colloids Surfaces B Biointerfaces* 2015;127:105–13.
- Phaechamud T, Yodkhum K, Charoenteeraboon J, Tabata Y. Chitosan–aluminum monostearate composite sponge dressing containing asiaticoside for wound healing and angiogenesis promotion in chronic wound. *Mater Sci Eng, C* 2015;50:210–25.
- Sathiyaseelan A, Shajahan A, Kalaichelvan PT, Kaviyaran V. Fungal chitosan based nanocomposites sponges – an alternative medicine for wound dressing. *Int J Biol Macromol* 2017;104:1905–15.
- Choi S, Chung MH. A review on the relationship between *Aloe vera* components and their biologic effects. *Semin Integr Med* 2003;1:53–62.
- Fox LT, Mazumder A, Dwivedi A, Gerber M, Plessis JD, Hamman JH. *In vitro* wound healing and cytotoxic activity of the gel and whole-leaf materials from selected aloe species. *J Ethnopharmacol* 2017;200:1–7.
- Chen H, Xing X, Tan H, Jia Y, Zhou T, Chen Y, et al. Covalently antibacterial alginate-chitosan hydrogel dressing integrated gelatin microspheres containing tetracycline hydrochloride for wound healing. *Mater Sci Eng, C* 2017;70:287–95.
- Alavarse AC, Oliveira Silva FW, Colquea JT, Silva VM, Prieto T, Venancio EC, et al. Tetracycline hydrochloride-loaded electrospun nano fibers mats based on PVA and chitosan for wound dressing. *Mater Sci Eng, C* 2017;77:271–81.
- Dhanavel S, Nivethaa EAK, Narayanan V, Stephen A. *In vitro* cytotoxicity study of dual drug loaded chitosan/palladium nanocomposite towards HT-29 cancer cells. *Mater Sci Eng, C* 2017;75:1399–410.
- Liu K, Peng-cheng K, Liu R, Wu X. Dual AO/EB staining to detect apoptosis in osteosarcoma cells compared with flow cytometry. *Med Sci Monit Basic Res* 2015:15–20.
- Mekahlia S, Bouzid B. Chitosan-Copper (II) complex as antibacterial agent : synthesis, characterization and coordinating bond- activity correlation study. *Phys Procedia* 2009;2:1045–53.
- Silverstein RM, Webster FX. Spectrometric identification of organic compounds, 6th ed. New York, NY, USA: John Wiley and Sons; 1997. p. 1–496.
- Di Mario F, Rapanà P, Tomati U, Galli E. Chitin and chitosan from Basidiomycetes. *Int J Biol Macromol* 2008;43:8–12.
- Gunasekaran S. Qualitative analysis on the infrared bands of tetracycline and ampicillin. *Proc Indian Natl Sci Acad Part A* 1996;62(4):309–16.
- Abdulghani AJ, Jasim HH, Hassan AS. Determination of tetracycline in pharmaceutical preparation by molecular and atomic absorption spectrophotometry and high performance liquid chromatography via complex formation with Au (III) and Hg (II) ions in solutions. *Int J Anal Chem* 2013;2013:1–11.
- Cortes GKDR, Vieira EFS, Cestari AR, Chagas RA. Tetracycline release from chitosan/fish-scale-based membranes. *J Appl Polym Sci* 2014;131:1–7.
- Niederhofer A, Müller BW. A method for direct preparation of chitosan with low molecular weight from fungi. *Eur J Pharm Biopharm* 2004;57:101–5.
- Shao W, Liu H, Wang S, Wu J, Huang M, Min H, et al. Controlled release and antibacterial activity of tetracycline hydrochloride-loaded bacterial cellulose composite membranes. *Carbohydr Polym* 2016;145:114–20.
- Liang D, Lu Z, Yang H, Gao J, Chen R. Novel asymmetric wetttable AgNPs/chitosan wound dressing: *in vitro* and *in vivo* evaluation. *ACS Appl Mater Interfaces* 2016;8:3958–68.
- Su C, Yang H, Song S, Lu B, Chen R. A magnetic superhydrophilic/oleophobic sponge for continuous oil-water separation. *Chem Eng J* 2016;309:366–73.
- Hajosch R, Suckfuell M, Oesser S, Ahlers M, Flechsenhar K, Schlosshauer B. A novel gelatin sponge for accelerated hemostasis. *J Biomed Mater Res – Part B Appl Biomater* 2010;94:372–9.
- Su C, Yang H, Zhao H, Liu Y, Chen R. Recyclable and biodegradable superhydrophobic and superoleophilic chitosan sponge for the effective removal of oily pollutants from water. *Chem Eng J* 2017;330:423–32.
- Lu Z, Gao J, He Q, Wu J, Liang D, Yang H, et al. Enhanced antibacterial and wound healing activities of microporous chitosan-Ag/ZnO composite dressing. *Carbohydr Polym* 2017;156:460–9.